INFRARED TRANSMISSION OF BARIUM TITANATE

By

KENNETH M. PROCTOR

Bachelor of Science

Central State College

Edmond, Oklahoma

1956

Submitted to the Faculty of the Graduate School of
the Oklahoma State University
in partial fulfillment of the requirements
for the degree of
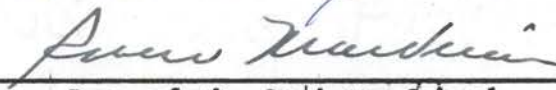MASTER OF SCIENCE
August, 1962

INFRARED TRANSMISSION OF BARIUM TITANATE

Thesis Approved:

_____
Thesis Adviser

_____

_____
Dean of the Graduate School

ii

ACKNOWLEDGMENT

TABLE OF CONTENTS

LIST OF TABLES

List of Figures

CHAPTER I

INTRODUCTION

Crystalline Phases of Barium Titanate

Barium titanate is a clear yellow, translucent material which is
ferroelectric below the Curie point at 120°C. Its crystalline symmetry
has been discussed by Megaw (1). At higher temperatures the crystal
system is cubic, having the typical perovskite (calcium titanate)
structure. Figure 1 illustrates this crystalline structure. Below the
Curie point the structure is tetragonal. It is easiest to visualize
this structure as derived from the cubic by stretching it slightly par-
allel to one cube edge and releasing all atoms from their special
positions so that they can have small displacements in this direction.
The axial ratio is about 1.01. Crystal domains are formed which can be
observed under a polarizing microscope.

Below 0°C the structure may be pictured as derived from the original
cube by stretching it along one face diagonal and compressing it along
the other, these diagonals becoming the new orthorhombic axes. The
third axis retains its original direction but suffers a slight change
of relative length. Hysteresis is observed in this phase change.

Below a temperature of from -70°C to -90°C, the crystal changes
form again, this time taking on a rhombohedral structure. This structure
is visualized by stretching the original cube along a body diagonal, that
is, along a line joining opposite corners of the cube. An even greater

1

Barium ⬡   Oxygen ◯   Titanium ●
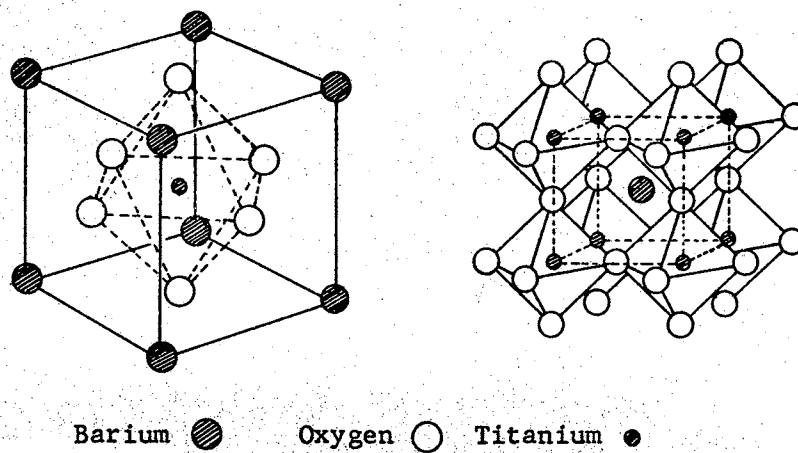
Figure 1. The Ideal Perovskite Structure.
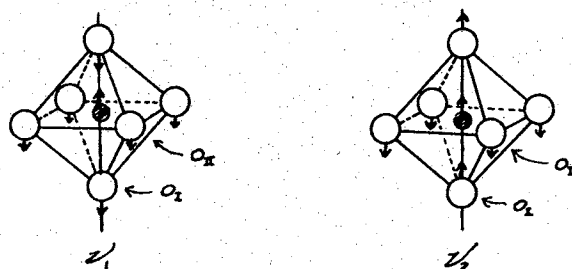
Figure 2. The F_{1u} Vibrations of the Oxygen Octahedron.

hysteresis is observed in this phase change.

It was the purpose of the present investigation to study the optical transmission of this material in its various phases. Much information about the crystalline structure may be found from the infrared transmission since it is in this region of the spectrum that the fundamental vibrations of the atoms occur. It is also important to obtain the short wavelength cutoff or absorption edge of the material since this provides one with a value for the optical forbidden energy gap which may be compared to the value obtained by electrical conductivity measurements.

Results Obtained by Previous Investigators

Mara et al. (2), Hilsum (3), and Yatsenko (4) have reported room temperature transmission curves of crystals of barium titanate showing an absorption at 8 microns, a long wavelength cutoff at about 11 or 12 microns, and a short wavelength absorption edge at 0.4 microns.

Horie et al. (5,6) have studied the temperature dependence of the absorption edge. From 150°C down to -70°C, it shifts from 0.42 to 0.39 microns. At the lower crystal transition point there is a discontinuity, the edge shifting abruptly back to 0.42 microns. At the same time the transmission above the edge decreases. This shift shows hysteresis. They also observed the transmission at 0.50 microns with polarized and unpolarized light. With unpolarized light the transmission was observed to change abruptly at the 0° and -80° transitions, showing hysteresis. With polarized light a change at 120° was also observed in mixed domain crystals, but only at 0° and -80° in single c-domain crystals. An explanation in terms of crystal optics of the domain structure is given.

With the ordinary single crystals having a thickness of from 0.05

to 0.1 mm, the infrared cutoff occurs at about 12 microns (850 cm^{-1}). Since these samples are too thick for their spectra to be observed in the far infrared, many workers resort to powdered samples.

Mara et al. (2), obtained two broad dips at 550 cm^{-1} and beyond 300 cm^{-1}. They observed no change in the higher frequency band in going from the cubic structure to the tetragonal structure. Megaw had stated that this phase transition would change the Ti-O bonding which should show up as a shift in this band. However, this is probably due to the wide temperature range of the phase transitions in a powdered sample (See below).

Yatsenko (4) also reports a broad absorption at about 600 cm^{-1} (16-17 microns). (In a later article (7) he reports bands at 578 cm^{-1} and 410 cm^{-1}.) He states that this 600 cm^{-1} absorption is due to the vibrations of the Ti ion in the oxygen octahedron and that the 8 micron absorption one obtains with a single crystal is the first overtone of this fundamental vibration. However, for a single crystal, this fundamental vibration is at 20 microns, not 16 microns (8).

Last (8) reports absorptions at 540 and 400 cm^{-1} using a powdered sample. He states that the phase transitions in the powdered samples cover a wide temperature range. For this reason very thin single crystals were prepared by a special etching technique (9). The crystals were etched in hot phosphoric acid above the Curie temperature until they were about 0.0015 mm thick. Measurements on these very thin crystals could then be carried out to 400 cm^{-1}. Lack of sufficient energy prevented observations at longer wavelengths so that only the higher frequency absorption was observed. For cubic barium titanate (T>120°C) the band is centered at 495 cm^{-1}. Below the Curie point where the crystal

is tetragonal, the band center depends on the domain arrangement. If the polar axis is normal to the crystal face the band is centered at 495 cm^{-1}. For a mixed domain crystal the center lies between 495 and 510 cm^{-1}, depending on the domain configuration. Observations were made on a poled crystal at room temperature. The band is centered at 495 and 517 cm^{-1} with the electric vector respectively perpendicular and parallel to the polar ("c") axis.

In the temperature range from 0° to -70°C where the crystal is orthorhombic, the band is centered at 520 cm^{-1} with a shoulder at 495 cm^{-1}. In the rhombohedral phase, below -70°C, the band becomes doubled with centers at 530 and 490 cm^{-1}.

Last's results are only shown from 800 to 450 cm^{-1}. Presumably these crystals were so thin that the weak absorption at 8 microns (1250 cm^{-1}) would not be observable. No mention is made of measurements made at various temperatures with non-etched crystals.

Normal Vibrations of the Perovskite Lattice

An extensive body of theoretical and experimental evidence indicates that the absorption bands in the infrared spectra of solids are caused by excitation of optically active vibrations. In order to interpret these spectra, one can study the vibrations as wave motions in periodic structures. A qualitative development of the complete vibrational spectrum of a cubic perovskite crystal will be given in this section and the requirements for modes which can be excited by infrared radiation indicated. This development and the confirming experimental results are from Last's article (8).

The general form of the infrared vibrations can be determined by

the use of lattice-symmetry arguments. A crystal of BaTiO$_3$ containing N unit cells, each with 5 atoms, has 15N degrees of freedom. Of these 15N modes, there are 3N degrees of freedom related to translational motion and 3N to torsional motion of the unit cell. The remaining 9N modes are associated with vibrational degrees of freedom.

In the Born-von Karman treatment of lattice vibrations, it is shown that each normal mode of a unit cell corresponds to N normal modes of the crystal, the wavelength associated with the lattice vibration determining the phase shift between adjacent unit cells. In the case of optically active vibrations, the phase of the lattice vibration must match that of the exciting electromagnetic wave. Since the unit-cell dimensions are extremely small compared to the exciting infrared wavelength, the phase shift between neighboring cells is negligible and all equivalent atoms in the lattice can be considered to vibrate in phase. A discussion of the vibrational frequencies of the unit cell will thus give information equivalent to one of the vibrational frequencies of the complete lattice.

The nine vibrations of the unit cell can be classified by division into three vibrations of the Ba against the TiO$_3$ group, and six internal TiO$_3$ vibrations. The interactions between these motions depend upon the masses and restoring forces of the vibrating atoms, and can be expected to be small in the case of BaTiO$_3$. The Ba-(TiO$_3$) vibrations can be treated by considering the TiO$_3$ group as a single atom situated at the Ti position, and the vibrational problem that of a diatomic crystal of equivalent structure (e.g., the CsCl structure). In the cubic phase this will lead to a triply degenerate vibration since three equivalent axes exist. A low frequency band, designated by v_3, will be assigned to this

Ba-(TiO_3) vibration. This frequency occurs outside the range of observation, but is calculated from specific heat data to be about 225 cm^{-1}.

In discussing the vibrational nature of the TiO_3 group, it is considered to be arranged as a central Ti atom octahedrally surrounded by six O half-atoms, to give the group the correct symmetry properties. This octahedron has the symmetry of the point group O_h, which has the six species of the normal vibrations, A_{1g}, E_g, F_{1u}, F_{1u}, F_{2u}, F_{2u}, F_{2g}, as discussed by Herzberg.

The requirement that atoms in equivalent positions in neighboring cells must perform the same vibrational motion reduces this set of normal vibrations to the two infrared-active vibrations of the species F_{1u}. The infrared-inactive vibrations of the species F_{2u} are related to the torsional motion of the unit cell.

If a vertical axis is chosen through a Ti-O chain, the two O half-atoms lying along this chain labeled O_I, and the four half-atoms at right angles to this axis O_{II}, the two F_{1u} normal vibrations can be illustrated as shown in Figure 2. In the first, a "stretching" vibration, the motion is primarily that of a change in length of the Ti-O_I bond. The frequency of this vibration is designated as v_1. In the second, a "bending" vibration, the motion is that of a change in the O_{II}-Ti-O_I bond angle. The frequency of this vibration is designated by v_2. Both the relative magnitude and sign of the displacements will depend on the bond-force constants and relative masses of the atoms. Since three equivalent axes exist in the case of the cubic lattice, these vibrations will both be triply degenerate. For a single crystal in the cubic phase, band v_1 is centered at 495 cm^{-1}. Band v_2 cannot be measured using a single crystal, but from the results of powdered samples it may be estimated to be 340 cm^{-1}. This

value is probably accurate to within 25 cm^{-1}.

The degree of degeneracy of these two bands in structures of lower symmetry may be determined by resolving the symmetry types of the cubic point group into point groups of lower symmetry, as shown in Table 1. The cubic triple degeneracy is partially removed in the tetragonal structure and each of the bands is doubled. This is easily visualized since the Ti-O distance along the polar axis is greater, while the interionic distances of the two vibrations at right angles to the polar axis are the same. In the orthorhombic structure the degeneracy is completely removed and each band is tripled. The symmetry species present in the rhombohedral structure are the same as those of the tetragonal structure and the bands are again doubled. Thus, three triply degenerate infrared-active vibration bands are expected in the spectrum of cubic barium titanate, with the degeneracies partially or completely removed in the phases of lower symmetry.

TABLE I

CRYSTAL SYMMETRY AND REARRANGEMENT OF SYMMETRY
SPECIES FOR THE FOUR PHASES OF $BaTiO_3$

Symmetry	Point Group	Species			Expected Band Structure
Cubic (>120°C)	O_h		F_{1u}		Single
Tetragonal (5° to 120°)	C_{4v}		E	A_1	Double
Orthorhombic (-80° to 5°)	C_{2v}	B_1	B_2	A_1	Triple
Rhombohedral (<-80°)	C_{3v}		E	A_1	Double

The effect on the spectrum of the symmetry changes occurring at the various phase transitions will now be discussed. The comparison of primary interest is that of the cubic and tetragonal spectra, since the material becomes ferroelectric when it undergoes the transition to the tetragonal state. The slightly broader band in the tetragonal spectrum is expected since this band is now doubly rather than triply degenerate. The band intensities are equal for the cubic and tetragonal phases. This indicates that the frequency difference between vibrations parallel and at right angles to the polar axis is slight; if one of the components of the tetragonal band experienced a large frequency change at the transition, it would shift out of the range of observation (since it is not observed) and the band intensity would decrease markedly upon transition. Measurements of the maximum absorption while the temperature was slowly lowered through the Curie point indicate no anomalous intensity jump not explainable by the slight shift of band center.

The polarized-light measurements on the tetragonal crystal show that the vibrational frequency along the polar axis is about 20 cm^{-1} higher than that at right angles to the polar axis. Since the unit cell is about 1% longer along the polar axis, this seems to violate the general rule that the vibrational frequency decreases when the bond distance is increased. However, as shown by x-ray and neutron-diffraction measurements, the Ti ion is displaced in the tetragonal phase to a noncentral position in the oxygen octahedron, so that there are two $Ti-O_I$ distances of 1.87 and 2.17 Å along the polar axis, as compared to the $Ti-O_{II}$ distance of 1.997 Å at right angles to the polar axis. The force constant receives its major contribution from short-order, closed shell repulsive forces rather than from Coulomb-attractive forces at the ionic equilibrium

positions. The force constant will therefore be more sensitive to a decrease of bond length than to an increase, and although there is a net increase in the average bond distance along the polar axis when $BaTiO_3$ becomes tetragonal, the greater effect of decreasing one bond increases the over-all force constant and thus the vibrational frequency. The Ti-O distance at right angles to the polar axis is practically the same as the Ti-O distance of 2.004 Å in the cubic phase. The fact that the same vibrational frequency of 495 cm^{-1} has been observed for each of these vibrations indicates that no large rearrangement of charge takes place at right angles to the polar axis when $BaTiO_3$ becomes tetragonal.

The symmetry arguments advanced earlier predicted that the band degeneracy should be completely removed in the orthorhombic phase and that the band should be tripled. However, two of the unit-cell dimensions are practically the same, and the slight frequency difference between these vibrations cannot be resolved. The rhombohedral band has the same double degeneracy as the tetragonal band, and a double absorption band is observed as expected. The centers of these bands occur at 530 and 490 cm^{-1}.

Purpose of the Present Investigation

A fairly complete study of the far infrared transmission and of the absorption edge of barium titanate in its various crystalline phases has thus been made by previous workers. These are, of course, the most important areas of investigation. However, no similar report has been found in the literature covering the optical properties in the wavelength region between these extremes. It was mainly this portion of the spectrum with which this investigation was concerned. Combinations of the

fundamental vibrational modes may produce absorption bands lying in this region of the spectrum. Even the infrared-inactive modes may combine in this manner to produce a higher frequency infrared-active mode. By selection rules it may be shown which combinations are possible. Not all of these absorptions will be seen however, since they may be to weak to be observable. An effort was made to find combinations which would produce the results obtained in this work. From this it was hoped a check could be made of Last's calculated values of ν_2 and ν_3.

CHAPTER II

INSTRUMENTATION AND MEASUREMENT TECHNIQUES

Instrumentation

The optical transmission measurements from 0.185 to 0.350 microns were taken by means of the Beckman DK-1 Spectrophotometer. This double beam instrument thus has an operating range covering the ultraviolet, the visible, and the near infrared regions of the spectrum. It has been described previously (10). In this study only room temperature measurements were taken using this instrument.

Measurements in the infrared region were made with the Beckman IR-7 Spectrophotometer. It is a double beam instrument having an operating range of 2.5 to 16 microns. By means of the long wavelength adaption unit the range of this instrument can be extended into the far infrared to 50 microns. Radiation from a Nernst glower source is split alternately into two beams, one being the sample beam and one the reference beam. In this manner the atmospheric absorptions are cancelled out. The beams are realigned alternately in space after passing through the sample compartment and then undergo three separate dispersions by a prism and grating system. From this spread spectrum, one narrow band of energy passes through the exit slit to the thermocouple for detection. An unequal energy in the sample and reference pulse will cause an optical attenuator or comb in the reference path to move, restoring beam balance. This null searching indicates the transmittance of the sample, and this information

is transmitted electrically to the recorder. At certain points in the spectrum atmospheric absorption will cause the energy from both pulses to be zero. To keep the recorder from drifting at these points a very small balancing signal is always present. Ordinarily when there is sufficient beam energy this balancing signal is overridden. In this manner when the pen reaches these points of atmospheric absorption it coasts on by without drifting.

For room temperature measurements use was made of the microbeam condenser. This accessory utilizes potassium bromide optics to focus the light beam into a small area and then spreads it out into a parallel beam again. By the use of this accessory the transmission of small samples may be measured. When used, the sample beam energy is less than that of the reference beam. In order to balance the recorder at 100% the reference beam must be attenuated. To do this a device was built consisting of a camera diaphragm and frame into which could be placed a wire screen. In this way the reference beam energy is continuously adjustable.

For high temperature measurements a special cell was constructed which could be used in conjunction with the microbeam condenser. For low temperature measurements it was difficult to design a cell which would fit into the beam condenser. Also, any condensation of water vapor would damage its lenses. Fortunately the samples of barium titanate were large and clear enough so that transmission measurements could be made without the use of this accessory, the results at least being sufficiently accurate for comparison purposes.

<center>Preparation of Samples</center>

The samples were grown by Northrip using the Remeika (11) method.

In brief the method consists of preparing a flux of potassium fluoride and barium titanate powder. The crystal growth has more success if iron oxide is added also, although if iron-free samples are desired this is left out. If an excess of barium is desired, one also adds barium nitrate. The mixture is melted and held at a temperature of 1200°C for a period of 3 to 6 hours and then allowed to cool at a rate of 5 to 20 degrees per hour until it reaches a temperature of 900°C. The molten flux is then poured off and the barium titanate crystals are found in the bottom of the crucible. The crystals grow in a "butterfly" formation.

Of the samples used in this investigation, XV and VIII are pure barium titanate crystals, while II has excess iron, and X and XIII have an excess of barium. Before and after any measurement a crystal was washed in acetone followed by a rinse in methyl alcohol.

<center>High Temperature Apparatus</center>

The high temperature apparatus (Figures 3a, 3b) consists of a small brass box with sodium chloride windows. This box is supported by rods such that it may be mounted crosswise in the beam of the microbeam condenser. When in use the box is evacuated so that the heat conducted to it will be a minimum. The top of the box is removable, a neoprene gasket forming the junction between the two parts. The heater assembly is attached to this top piece and a ceramic seal is used for the thermocouple and heater wires. Phosphor bronze clips hold the sample in place. Since a teflon ring is used to hold the heater assembly in place, the maximum operating temperature of the apparatus is limited by the possible emission of noxious fumes. The operating temperature should not exceed 200°C.

Rheostats are used to control the current to the heater coil so that

a steady temperature may be maintained. The temperature is read out on a potentiometer by means of a copper-constantan thermocouple affixed to the sample mount. In practice, a room temperature curve was first obtained and then runs above and below the Curie transition point at 120°C were carried out.

A great deal of difficulty was initially experienced with the high temperature apparatus. A light grease would deposit on the inside of the sodium chloride windows causing very strong absorptions at 2860 and 2930 cm^{-1}. Small absorptions at 1380 and 1465 cm^{-1} were also obtained. Since these absorptions became stronger each time the apparatus was used, they could not be ignored. The trouble was finally removed by the following procedure. Glass windows (which could be cleaned) were placed on the cell. Under vacuum conditions the heater was adjusted to about 150°C. The following day the grease would be cleaned off the windows. After repeating this procedure a number of times, no more grease was deposited and sodium chloride windows were put back on the cell. Subsequently no more trouble was experienced although small dips could still be seen at 2860 and 2930 cm^{-1} due to traces of the grease continually being deposited on the windows. It is reasonably certain at this time that this grease came about from either degassing of the brass cell or from the teflon heater assembly mount.
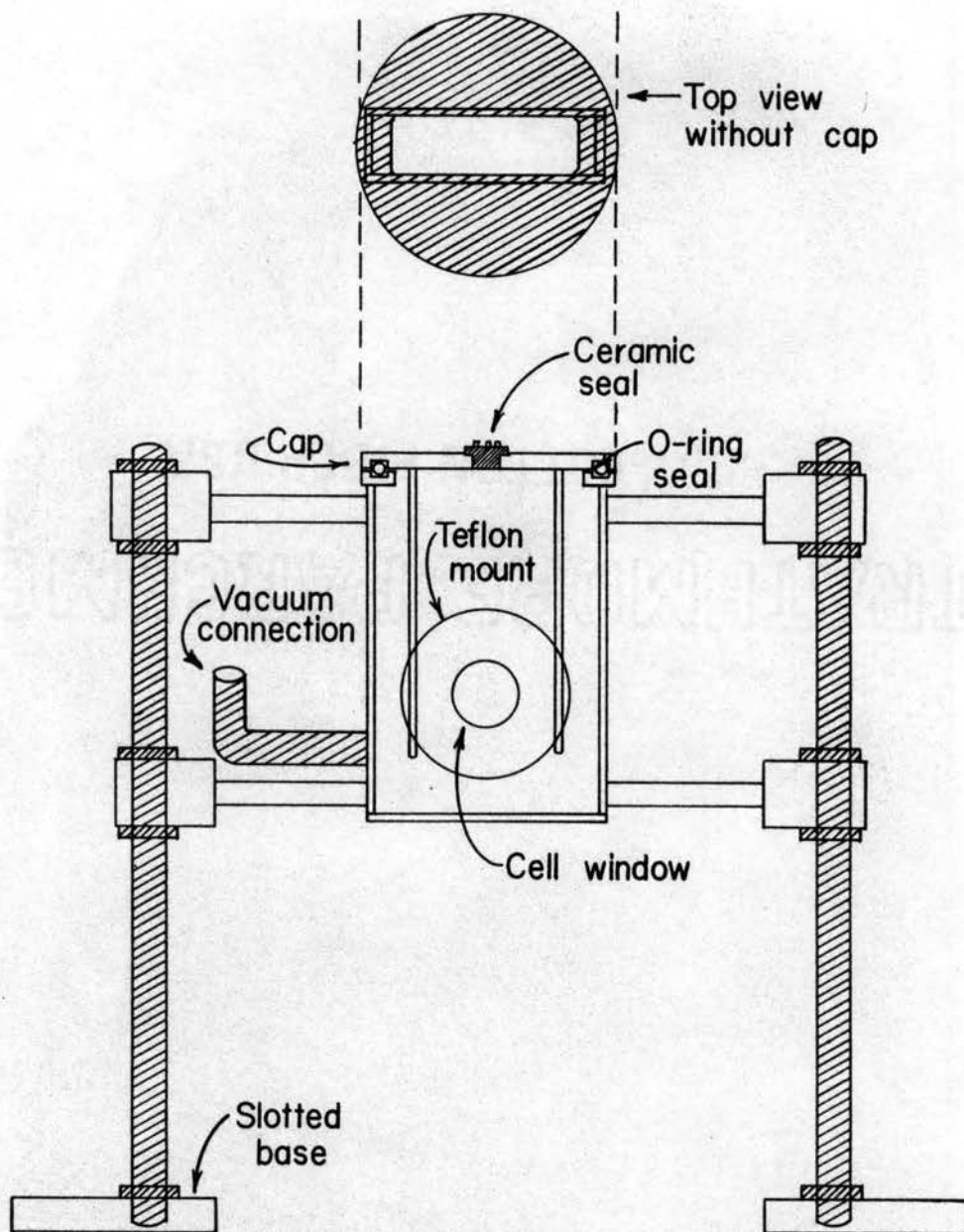
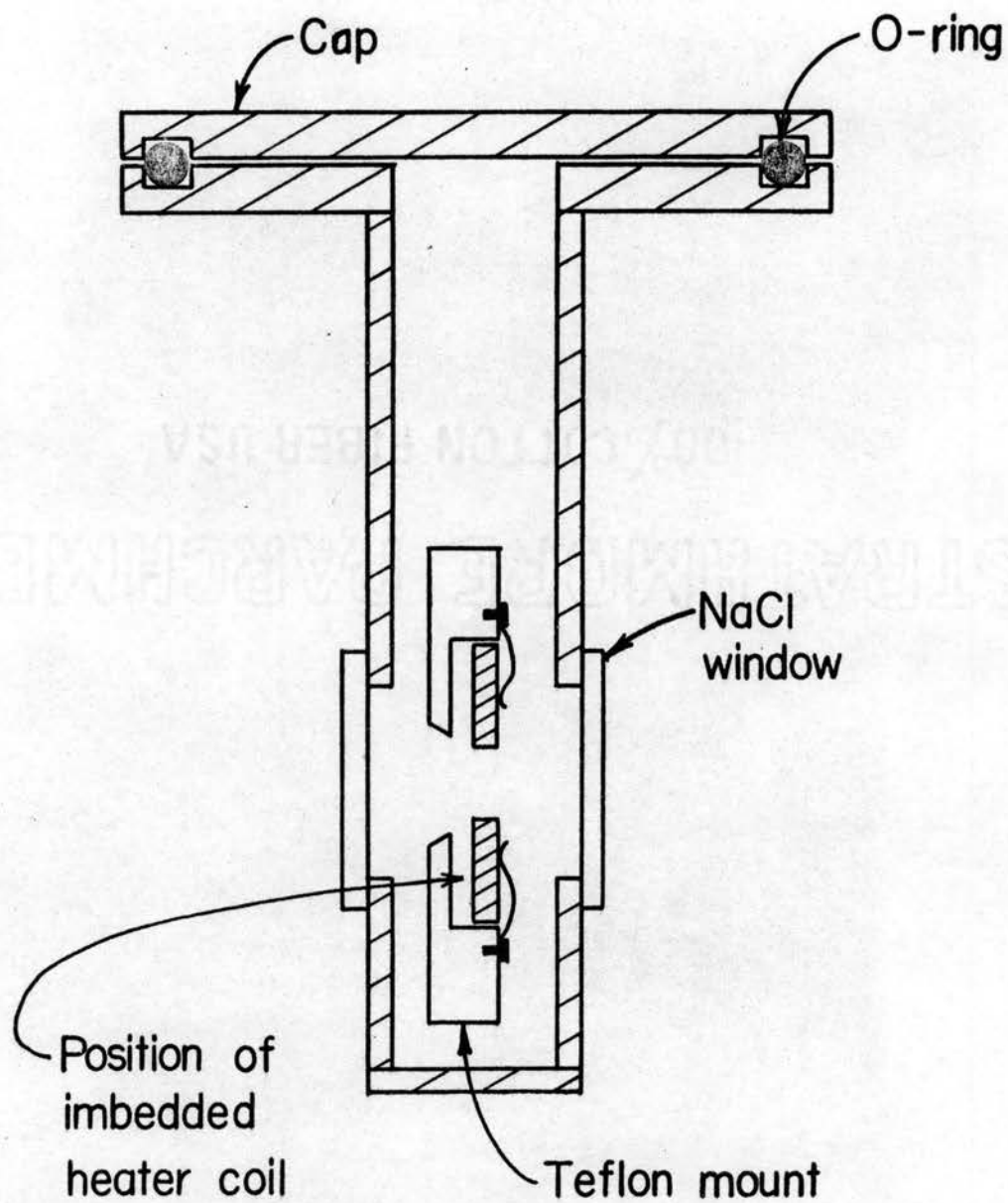Figure 3a. The High Temperature Apparatus.

Figure 3b. Cutaway View of the High Temperature Apparatus.

Low Temperature Apparatus

The low temperature apparatus is shown in Figure 4. The problems of designing a low temperature apparatus small enough to fit into the microbeam condenser made it impractical to use this accessory for these measurements. Since the samples of barium titanate were fairly large and clear there was sufficient beam energy to obtain data for comparison to the results at room temperature. It would be advantageous in the future to design an apparatus which could be used in conjunction with the microbeam condenser since measurements could then be taken on smaller samples.

The low temperature apparatus presently used consists of an outer glass shell with sodium chloride windows and an inner cup of brass, the space between being evacuated. The bottom of the cup is of solid brass with a crosswise hole near the bottom, through which the beam of light passes. A brass ring upon which the sample is mounted fits into this crosswise tube. A copper-constantan thermocouple is used for temperature measurement and a vacuum gauge is used to measure the pressure. Trouble was initially experienced in the use of this apparatus due to small leaks. At low temperatures water vapor would freeze onto the sample, completely masking the transmission measurements. The difficulty was removed when the leaks were repaired.

In use the apparatus was placed in the sample compartment of the IR-7 in a position such that the energy was maximum. The instrument was adjusted in the usual way. The sample compartment cover was then closed but the small door in the top of this cover left open. The top of the apparatus came through the opening. A frame of wood was held in place

on this opening by c-clamps. A flexible plastic cover with a hole in it was fastened to the frame. Rubber bands sealed this plastic cover around the glass envelope of the apparatus to prevent air from getting into the sample compartment. A rubber hose fitted into a hole in the plastic cover so that the compartment could be flooded with nitrogen. This prevented any moisture condensation inside the sample compartment. The space between the brass cup and glass envelope was then evacuated for insulation purposes. A cold trap was used in the vacuum line to help remove water vapor before cooling the cell. Liquid nitrogen was poured into the cup to cool the sample to the desired temperature. It was found that a small plug of cotton in the bottom of the cup helped in preventing drastic temperature fluctuations. At first a frozen liquid was used for this purpose but expansions caused leaks in the soldered joints in the bottom of the cup.

The following operating procedure was finally adopted. A room temperature curve was first obtained. Then the apparatus was cooled to about 10°C and another curve obtained. The instrument was then set at about 3 microns and the apparatus cooled again. A sudden lowering in transmission was observed at about 0°C, the crystal transition to ortho-rhombic form taking place at this temperature. The temperature was lowered to -5°C to be sure the transition was complete and another curve run. Transmission curves above and below the -90° transition point were obtained by following the same procedure. Another sudden decrease in transmission was obtained at this transition point.

After the data was completed with one sample the apparatus was allowed to warm to room temperature. Then air was let into the apparatus and the brass cup lifted out so that another sample could be inserted.

Stable temperatures were much more difficult to maintain than with the high temperature apparatus. Hence one does not dare make a run very close to the transition temperature. Otherwise one could cool the sample well beyond the transition point to be sure the transition was complete and then allow it to warm up again until the temperature was just below that of the transition point before making a run. However, a temperature difference of 10 or 15 degrees between runs made above and below a transition point is justifiable considering that there is a difference of 90 degrees between the low temperature transitions.
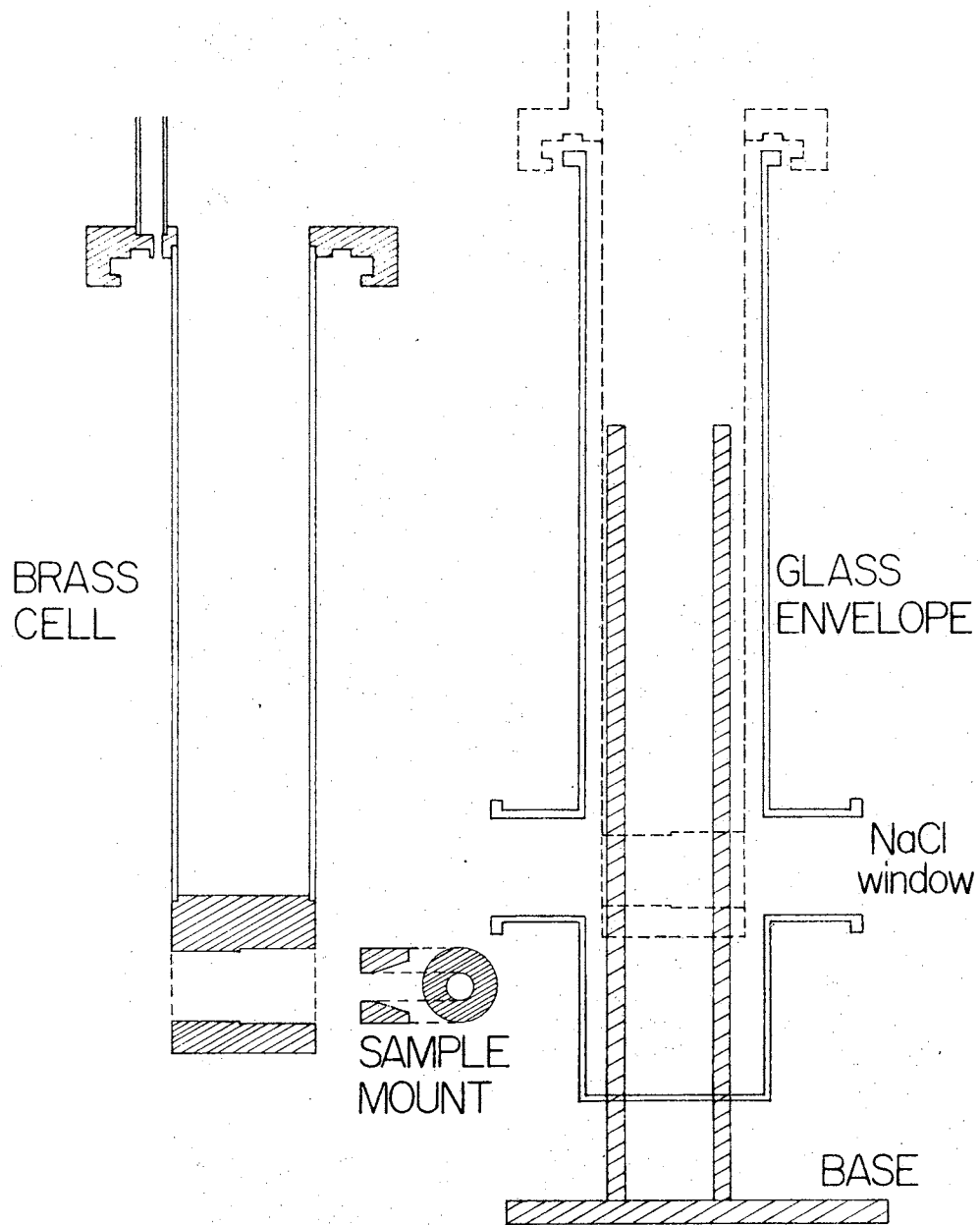
Figure 4. The Low Temperature Apparatus.

Reduction and Representation of Data

The transmission curves of several samples are shown in Figures 5-10. The data for plotting these curves was obtained from the DK-1 and IR-7 spectrophotometers. In reducing the data the first step is to correct the transmission spectrum for deviations of the 100% line. This is accomplished by dividing the transmission value of the sample by the transmission value of the 100% line and multiplying the result by 100. The data from both instruments is corrected in this manner. It will then be found that the high wavelength end of the DK-1 spectrum will indicate a lower transmission than the low wavelength end of the IR-7 spectrum (12). It is assumed that the IR-7 data is correct. In order to make the two sets of data match, one divides the transmission reading at 2.6 microns on the IR-7 by that on the DK-1. Then the DK-1 data is multiplied by this correction factor. Points are then plotted on graph paper and a curve traced through them. It will be noted that this data is plotted with respect to wavelength in microns. The IR-7 data is linear with respect to the frequency in wavenumbers. The reciprocal of this must be taken to obtain the wavelength in centimeters. Thus, these curves as drawn will have the effect of greatly compressing the DK-1 data and greatly expanding the IR-7 data. However, since the greatest interest lies in the portion of the spectrum covered by the IR-7, this is an advantage.

The transmission curves in Figures 11-14 are taken from a portion of the infrared spectrum. These curves were traced directly from the graph made by the IR-7 and are therefore not corrected for deviations of the 100% line. The transmission values indicated are not absolute. However, for comparison purposes this makes no difference and a more accurate curve may be obtained by this method.

CHAPTER III

RESULTS

Optical Properties at Room Temperature

A tabulation of the main results of the transmission curves for all
samples tested is given in Table II. The short wavelength cutoff was
taken to be the wavelength at which the spectrophotometer indicated zero
transmission through the sample. The cutoff value for the pure samples
was found to be 0.390 microns. This corresponds to an optical activation
energy of 3.18 ev.

The presence of a weak absorption band was recorded in the infrared
region at a wavelength of 8 microns. The samples with excess barium did
not show this absorption because of their greater thickness.

Figures 5-10 show the transmission spectrum at room temperature of
four representative samples of barium titanate. The 8 micron absorption
dip may be seen and an inflection in the curves at 1475 cm^{-1} (about 7
microns) should also be noted. Samples X and XIII also show inflections
near the low wavelength cutoff. These particular inflections may be
the result of impurities or may be due to scattering of the light by
these samples. The transmission curve of a sample of strontium titanate
is also shown. The sample used had a rather poor polish and it is
definitely felt the slope of the curve in the lower wavelength half of
the spectrum is due to scattering of the beam by the sample. When
a sample scatters the light excessively the indicated transmission level

becomes too low. This is particularly true of the DK-1 Spectrophotometer since there is a large distance between the sample and the detector. It would be advantageous to build a beam condenser for this instrument.

As noted in Table II, oscillations were superimposed on the transmission curves of four of the thinnest barium titanate samples throughout the infrared region. Figure 11 shows a portion of the infrared transmission curve of sample XVII, illustrating these oscillations. Following this an analysis in terms of interference fringes is given.

Transmission of all samples was also checked into the far infrared region making use of the CsI interchange on the IR-7 Spectrophotometer. All indicated zero transmission out to 36 microns.

TABLE II

TABULATION OF ROOM TEMPERATURE RESULTS

Sample	Short λ Cutoff (millimicrons)	IR Absorption (cm^{-1})	Long λ Cutoff (cm^{-1})
		Pure Samples	
XVI	389.5	1260	831 *
XVII	390	1257.5	832 *
XV	390	1250	857.5
VII	398.5	1248	867 *
I	399	1255	917.5
VI	401	1255	833 *
VIII	401.5	1255	990
V	406	1252	1028
		Excess Iron	
II	425	1253	1033
IV	432	1253	1045
III	436	1245	1088
		Excess Barium	
X	455	No dip	1308
IX	Not done	No dip	1382
XIV	456.5	No dip	1339
XIII	447	No dip	1325
XII	477.5	No dip	1385
XI	460	No dip	1356

*Oscillations were superimposed upon the IR transmission curves of these samples.
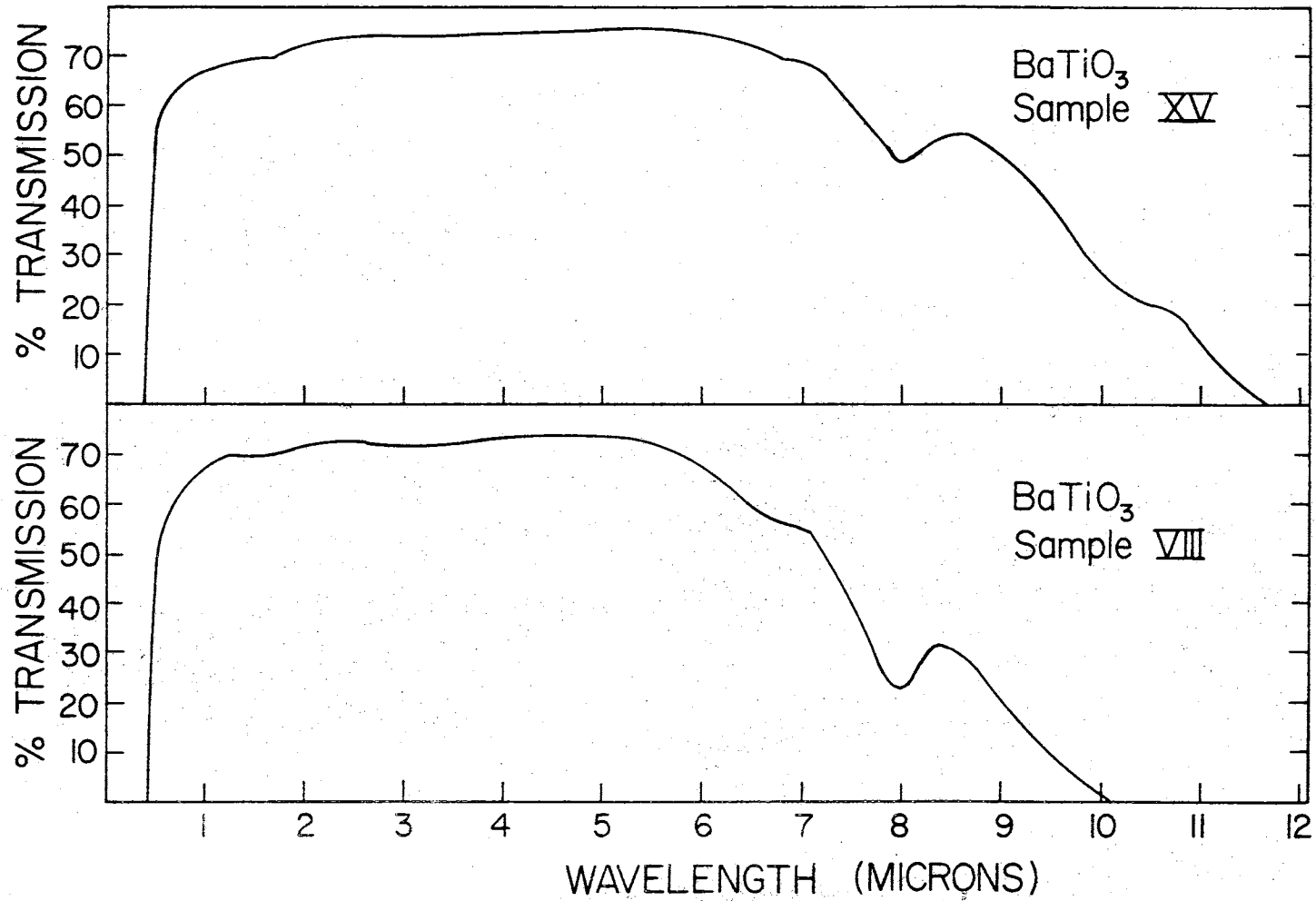
Figures 5 and 6
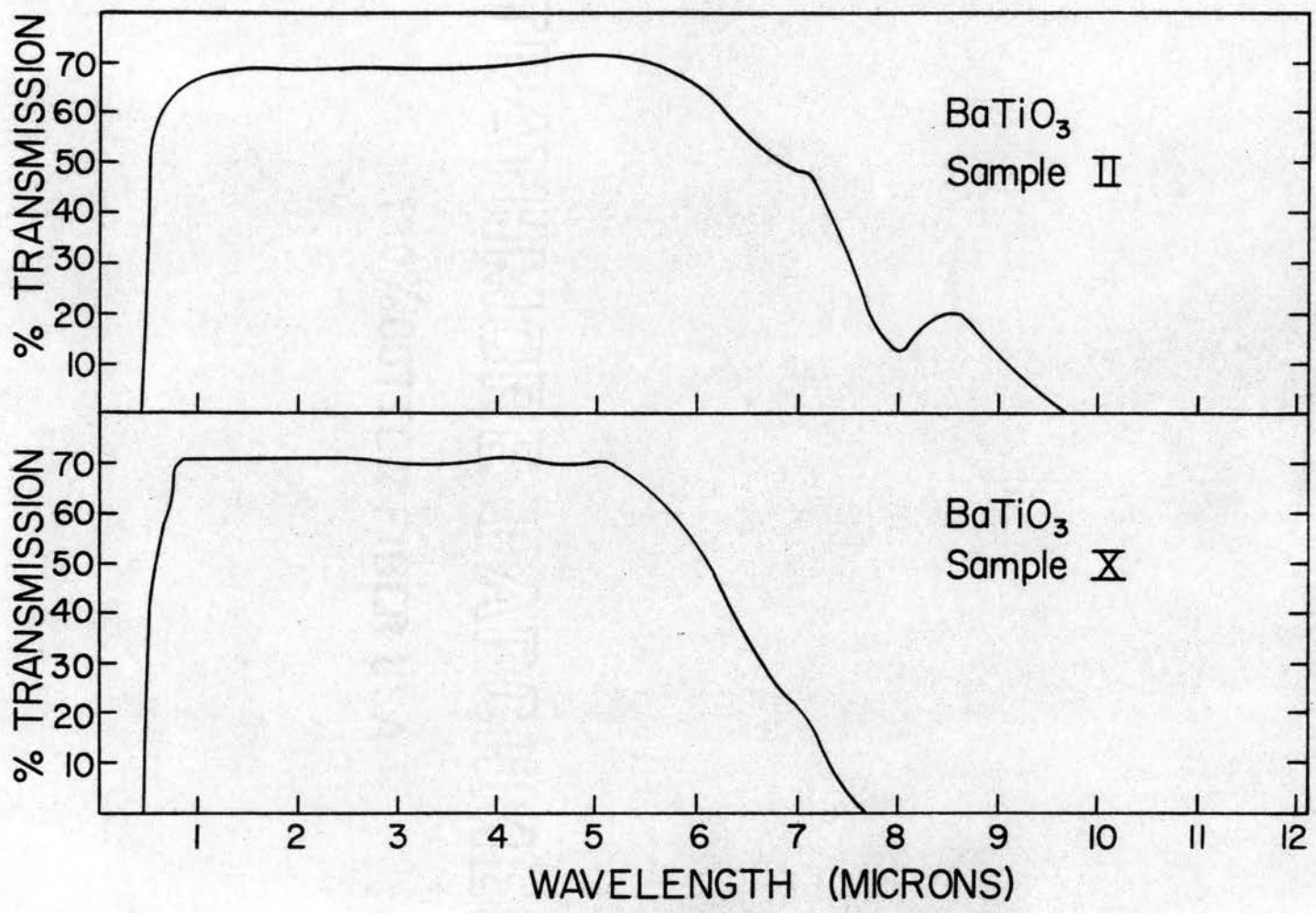
Figures 7 and 8

Figures 9 and 10

Interference Fringe Analysis

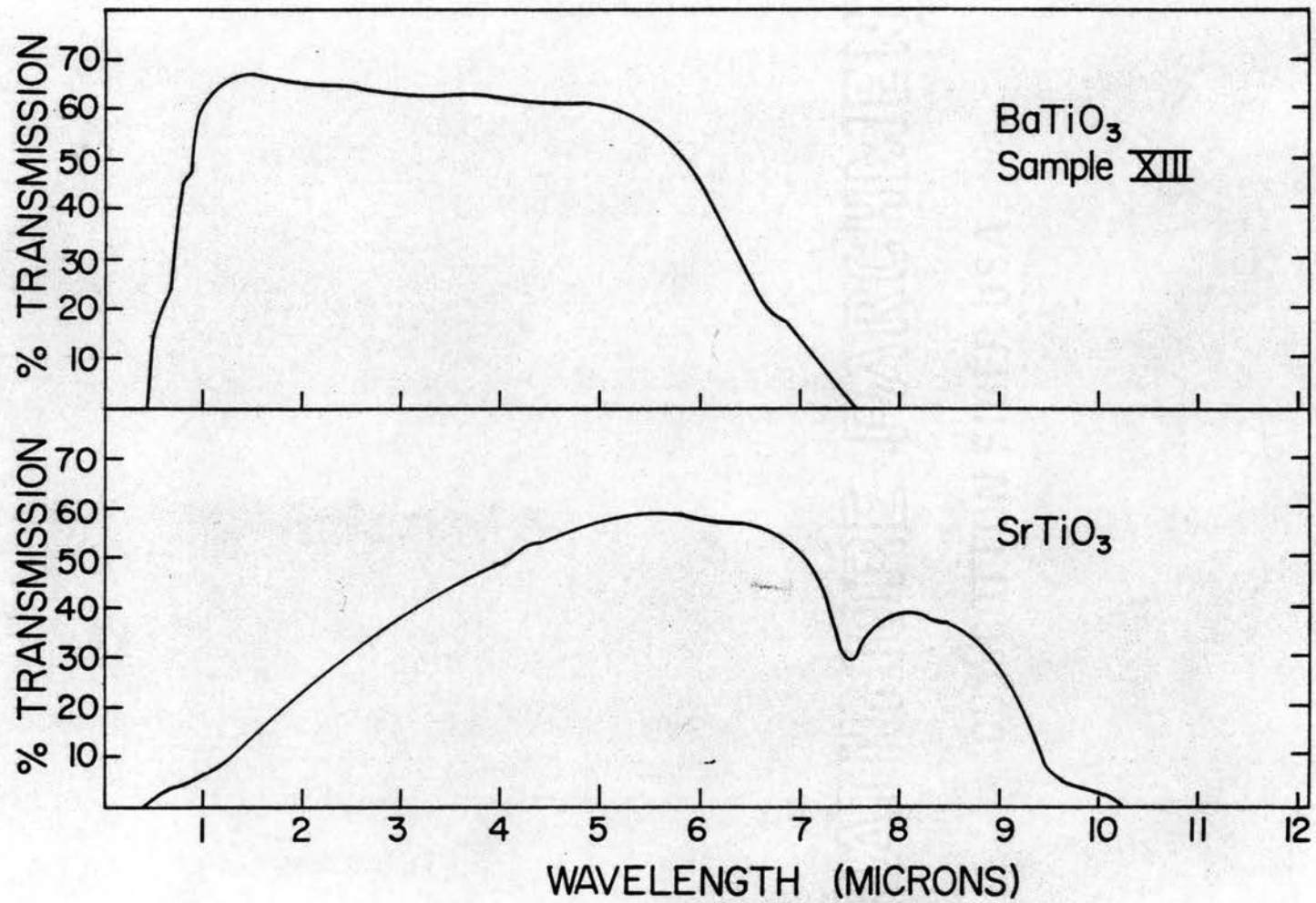The IR-7 transmission curves of several of the thinner samples had oscillations superimposed on them (Figure 11). These oscillations were caused by interference and had an amplitude of from 2 to 5 percent.

For a dark fringe,

$$\text{Path difference} = 2t = (N + \tfrac{1}{2})\lambda,$$

where N is an integer and t the thickness of the crystal. Adjacent fringes occur for

$$2t = (N - 1 + \tfrac{1}{2})\lambda_2 \text{ and } 2t = (N + \tfrac{1}{2})\lambda_1,$$

where $\lambda_2 > \lambda_1$. Eliminating N, one obtains

$$2t\,(1 - \lambda_1/\lambda_2) = \lambda_1.$$

These are wavelengths as measured in the medium. The index of refraction is

$$n = c/v = \lambda_{air}/\lambda_{med}$$

so that

$$\lambda_{med} = \lambda_{air}/n.$$

Thus, in terms of the wavelengths as measured in air,

$$2t\,(1 - \lambda_1/\lambda_2) = \lambda_1/n.$$

By definition, the wavenumber v is given by

$$v(\text{cm}^{-1}) = 1/\lambda(\text{cm}) = 10/\lambda(\text{mm}).$$

Thus, if t is in mm, we have

$$2t\,(1 - v_2/v_1) = 10/nv_1,$$

which becomes

$$t\,(\text{mm}) = \frac{5}{n}\,\frac{1}{\Delta v}.$$

At room temperature the index of refraction varies with direction in the crystal and the adjacent crystal domains are aligned differently.

However Merz (13) gives an average value for this quantity of 2.40. Since the difference between the two indices is only 0.055, this figure is sufficiently accurate. Using this value and measuring the average separation of fringes, the thicknesses of the crystals were calculated. These values are compared in Table III with values obtained using a traveling microscope. The comparison is good. Actually the calculated values are probably more accurate than those obtained with the microscope since the crystals are so thin. Last (8) obtained interference fringes also and used this method to measure the thickness of his crystals. His interference fringes occurred in the near infrared region of spectrum since he used samples etched down to a thickness of 0.0015 mm.

TABLE III

CRYSTAL THICKNESS DETERMINED BY INTERFERENCE

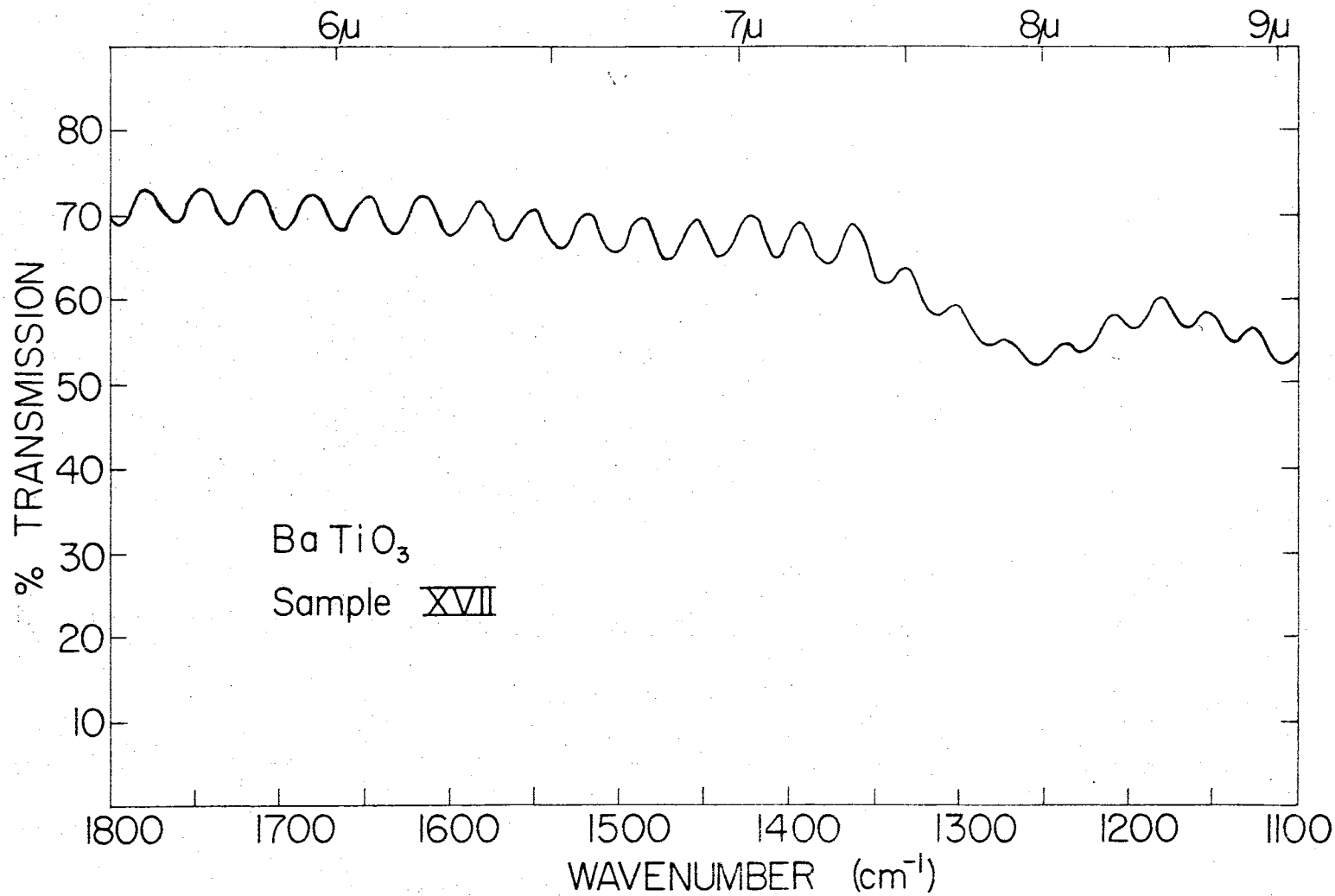| Crystal	Average $\Delta v(m^{-1})$	n	Calculated Value of t (mm)	Measured Value of t (mm)
XV	26.4	2.4	0.0789	0.0849
XVI	33.4	2.4	0.0624	Not available
VI	20.7	2.4	0.1007	0.1019
VII	25.9	2.4	0.0805	0.0831

Figure 11. Oscillations in the Spectrum of Sample XVII.

Variation of the Infrared Transmission with Temperature

The transmission characteristics of samples XV, VII, II, X, and XIII were studied at various temperatures throughout the infrared region above and below the crystal transition points. Figure 12 shows the transmission curve of a portion of the infrared region of sample VIII above and below the 0° C transition point. Figure 13 shows the transmission above and below the -90° C transition for this same sample. These figures show the shift to the left (shorter wavelengths) of the 1250 cm^{-1} band and also the appearance of a broad band at 1475 cm^{-1} in the lower transition phases. These results are typical of the other samples tested.

Differences above and below the Curie point (+120° C) were small. In going from the cubic to the tetragonal phase the left side of the 1250 cm^{-1} absorption is observed to shift slightly (from 1 to 5 cm^{-1}) to the right while the right side maintains its position. As the temperature is lowered through the tetragonal phase this band becomes slightly sharper and shifts very slightly (2 cm^{-1}) to the left. Also as the temperature is lowered from above the Curie point and on down through the tetragonal phase a slight flattening of the transmission curve in the 1475 cm^{-1} area may be seen.

When the samples change from the tetragonal to the orthorhombic phase (0° C) the over-all transmission at the left end of the infrared region (around 3 microns) is observed to suddenly decrease about 15 percent. There also occurs a shift of the 1250 cm^{-1} absorption band to the left (lower wavelength). This shift was 15 cm^{-1} for sample XV and 10 cm^{-1} for sample VIII. With sample XV this shift was more prominent on the left edge of the band. Also at this transition, the appearance of a broad absorption band at 1475 cm^{-1} is noted on all samples.

As the temperature is lowered through the orthorhombic phase the 1250 cm^{-1} band shifts further to the left by a small amount. Sample XV gave the greatest shift of 7 cm^{-1}. Samples VIII and II shifted only about 2 cm^{-1} although the absorption was obviously enhanced. The absorption at 1475 cm^{-1} was also somewhat enhanced.

When the rhombohedral phase was reached (about $-90°$ C), a sudden decrease in transmission again observed in the low wavelength end of the infrared range. The 1250 cm^{-1} band again shifted to the left. With sample XV this shift was 11 cm^{-1}, while with samples VIII and II the shift was 25 cm^{-1}. With all three samples the absorption was strongly enhanced. The 1475 cm^{-1} absorption was also strongly enhanced at this transition. This phase transition from orthorhombic to rhombohedral exhibited a great amount of hysteresis (over $20°$ C).
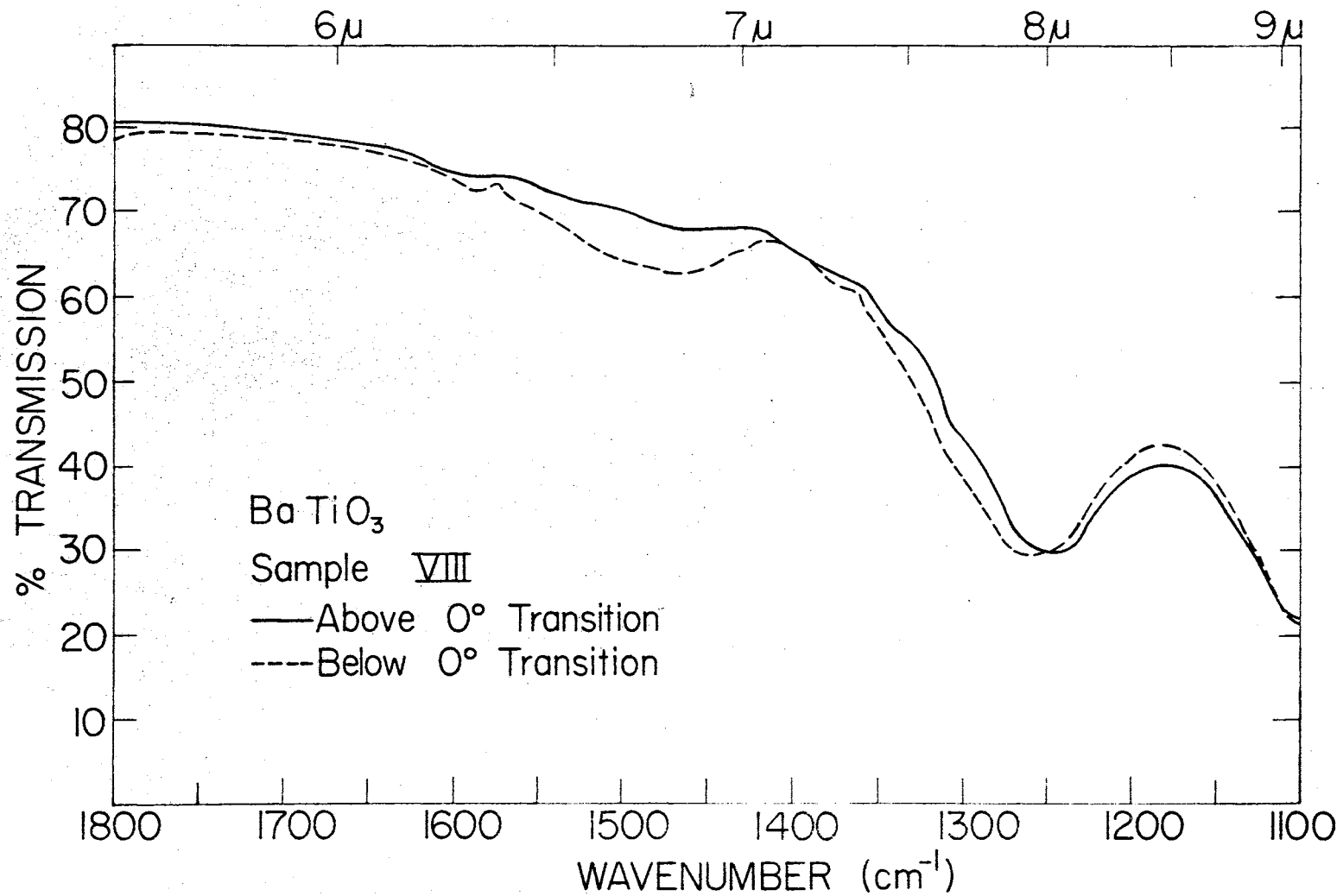
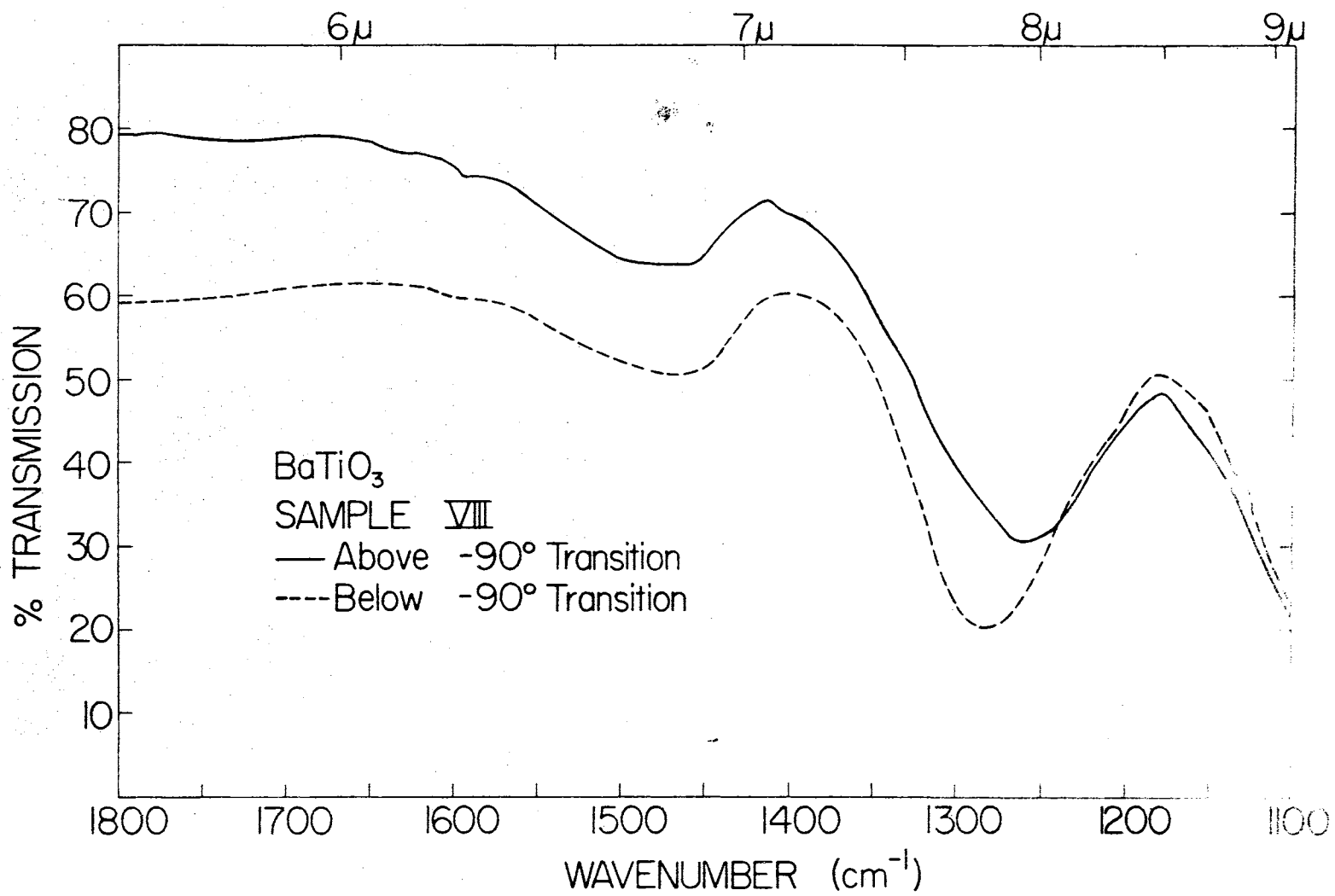Figure 12. Graph VIII Above and Below 0° Transition.

Figure 13.   Graph VIII Above and Below -90° Transition.

Results of Polarization Study

Two of the samples were poled with an electric field to align all of the domains along the same direction in the plane of the crystal. The effect could be checked with a polarizing microscope. The crystals were in the tetragonal phase and measurements were made at room temperature using the microbeam condenser and stacked-plate polarizer. The light beam first passes through the sample holder, which may be rotated; then through the polarizer, which passes only the horizontal component of the electric vector.

A comparison of results, with the electric vector perpendicular and parallel to the optical axis, is shown for sample II (Figure 14). With the electric vector perpendicular to the optical axis, the usual absorption dip occurs at 1250 cm^{-1}. When the electric vector is parallel to the optical axis, this absorption shifts to the left 37 cm^{-1} and is strengthened. Also another absorption appears centered at about 1492 cm^{-1}. No other differences were noted in the spectrum.

Sample II has a cutoff at 1033 cm^{-1}. Thinner samples show a fattening in the transmission curve at about 955 cm^{-1}. It was hoped that possible absorptions in this region could be studied using a poled crystal. However, no thin crystals of sufficient size were available and attempts at etching some of the larger samples were not too successful. The excellent technique of Last (9) of mounting the crystal between two pieces of a special teflon-silicone tape, preparatory to the etching process, would have made matters much simpler. However, this tape was not available in time to perform this experimentation. It is recommended that this tape be obtained for future work. Also some method of vibrating the crystal while it is suspended in the acid would help prevent

uneven etching caused by a white powder which was observed to form on
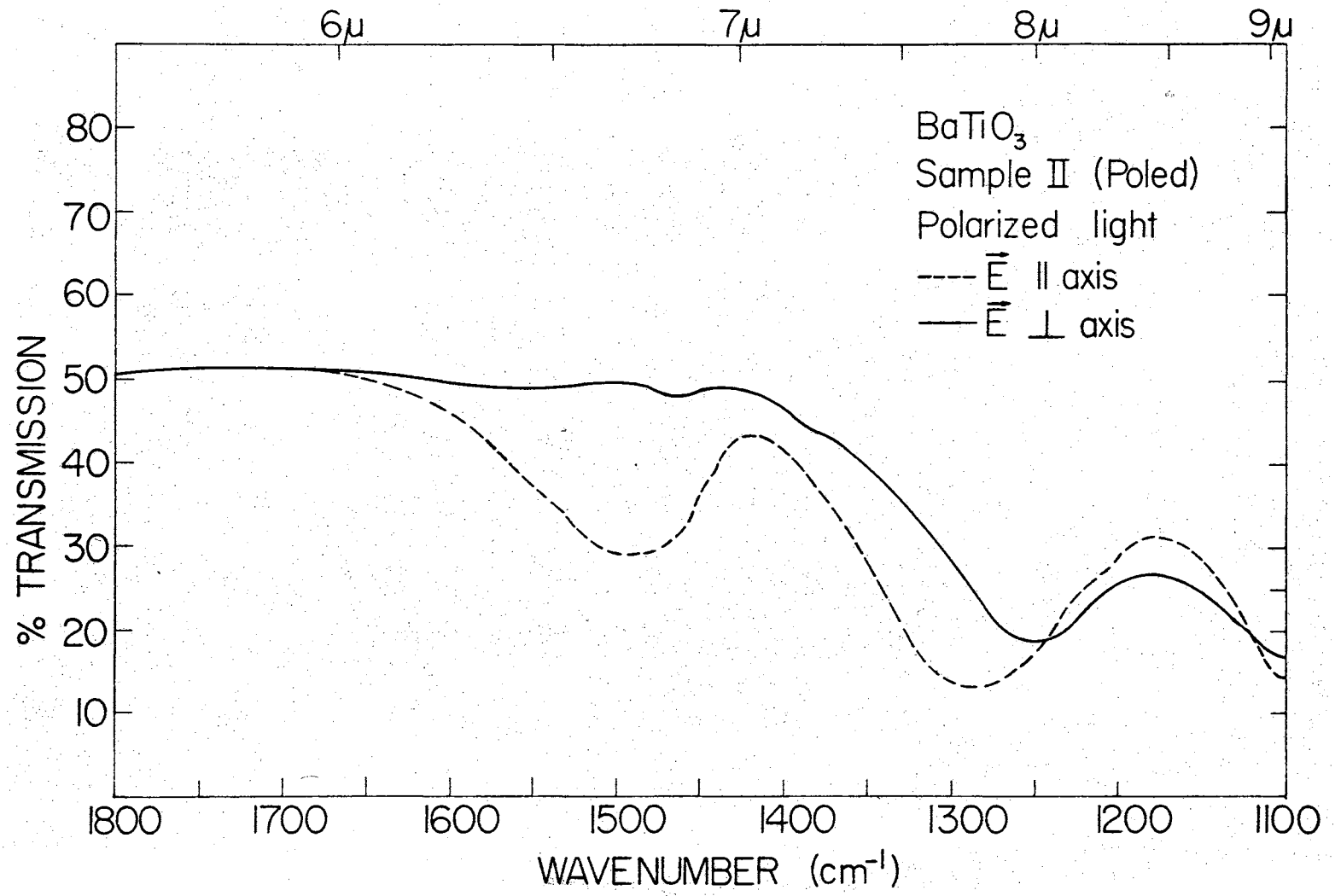the crystal during the etching process.

Figure 14.   Polarization Curves.

CHAPTER IV

CONCLUSIONS

Selection Rules

As stated in the introduction, combinations of the fundamental absorption frequencies may produce higher frequency absorption bands. From symmetry considerations selection rules may be obtained which can be used to show whether a suspected combination may occur (14,15). Barium titanate in the cubic form possesses O_h symmetry. It can be shown the allowed frequencies or combinations of these frequencies must be of the type F_{1u}. In the tetragonal form which has the C_{4v} symmetry, vibrations of types A_1 or E are allowed, the E vibration being doubly degenerate. The E vibration is excited under polarized light with the electric vector perpendicular to the crystal optic axis. Under this condition, a band centered at 1250 cm^{-1} was observed. With the electric vector parallel to the crystal axis bands were obtained at 1287 cm^{-1} and 1492 cm^{-1} which must possess the symmetry A_1. We may indicate these results as follows:

(cubic phase)   1250(F_{1u})

(tetragonal phase) 1250(E)   1287(A_1)   1492(A_1)

The values which shall be employed for the fundamental vibrations are:

v_1	v_2	v_3
$495(F_{1u})$	$320(F_{1u})$	$265(F_{1u})$
$517(A_1)$	$320(A_1)$	$265(A_1)$
$495(E)$	$320(E)$	$265(E)$

The values chosen for v_2 and v_3 differ from those given by Last, 340 and 225 cm^{-1}. This was done to give somewhat better agreement with the experimental results. Also the splitting of these bands in the tetragonal phase is ignored for lack of explicit information concerning values to be used for the particular symmetries. The magnitude of this splitting should be small however. Last's values for v_1 were obtained by direct experimental evidence and are considered conclusive.

The selection rules for combinations of the infrared-active modes are as follows:

O_h Symmetry

$F_{1x} \times F_{1u}$ (not allowed)	$(F_{1u})^2$ (not allowed)
$F_{1u} \times (F_{1u})^2 = F_{1u}$	$(F_{1u})^3 = F_{1u}$
$F_{1u} \times (F_{1u})^3$ (not allowed)	$(F_{1u})^4$ (not allowed)
$(F_{1u})^2 \times (F_{1u})^2$ (not allowed)	
$(F_{1u})^2 \times (F_{1u})^3 = F_{1u}$	

C_{4v} Symmetry

$A_1 \times A_1 = A_1$	$(A_1)^2 = A_1$
$A_1 \times E = E$	$(A_1)^3 = A_1$
$E \times E = A_1$	$(E)^2 = A_1$
$E \times (E)^2 = E$	$(E)^3 = E$

Combinations with infrared-inactive modes may also produce infrared-active modes, but these shall be ignored in this work. The frequencies of these infrared-inactive modes should be small.

As an example consider the second harmonic of the fundamental v_1 vibration in the cubic phase. This harmonic, 990 cm^{-1}, is not allowed. Even if it had been allowed this would not necessarily mean that it would be observed, since the absorption might be too weak. As another example consider the combination of the fundamentals, 517(A_1) and 320(E) in the tetragonal phase. This combination, 837 cm^{-1}, possesses E symmetry. This operation is indicated by the notation

$$517(A_1) + 320(E) = 837(E).$$

As another example,

$$517(A_1) + 2 \times 320E(A_1) = 1157(A_1).$$

The E following the number 320 indicates that the E mode of the 320 cm^{-1} band is being considered. The (A_1) following this indicates that the second harmonic of this frequency is of the type A_1. Then since $A_1 \times A_1 = A_1$, we obtain 1157(A_1), meaning there may exist an absorption at 1157 cm^{-1} having A_1 symmetry.

The most reasonable combinations of the fundamental infrared-active modes will be shown. The first line in each group refers to the cubic phase. If the result is denoted (F_{1u}), this indicates the combination is permissible. Following this, the combinations for the tetragonal phase are carried out.

$$(v_1 + v_1)$$

$$2 \times 495F_{1u} \qquad\qquad = 990 \text{ (not allowed}$$

$$495(E) + 495(E) \quad = 990(A_1)$$

$$495(E) + 517(A_1) \quad = 1012(E)$$

$$517(A_1) + 517(A_1) \quad = 1034(A_1)$$

$$(\nu_1 + 2\nu_1)$$

$$3 \times 495F_{1u} = 1485(F_{1u})$$

$$495(E) + 2 \times 495E(A_1) = 1485(E)$$

$$517(A_1) + 2 \times 495E(A_1) = 1507(A_1)$$

$$495(E) + 2 \times 517A_1(A_1) = 1529(E)$$

$$517(A_1) + 2 \times 517A_1(A_1) = 1551(A_1)$$

The first group was in a frequency range outside the primary region of observation. The second group, $(\nu_1 + 2\nu_1)$, indicates an absorption in the cubic phase at 1485 cm^{-1}. This absorption is evidently too weak to be observed except for a small flattening in this area. In the tetragonal phase there are two A_1 combinations and two E combinations, the latter not observed.

$$(\nu_1 + \nu_2)$$

$$495(F_{1u}) + 320(F_{1u}) = 815 \text{ (not allowed)}$$

$$495(E) + 320(A_1) = 815(E)$$

$$495(E) + 320(E) = 815(A_1)$$

$$517(A_1) + 320(E) = 837(E)$$

$$517(A_1) + 320(A_1) = 837(A_1)$$

$$(\nu_1 + 2\nu_2)$$

$$495(F_{1u}) + 2 \times 320F_{1u} = 1135(F_{1u})$$

$$495(E) + 2 \times 320A_1(A_1) = 1135(E)$$

$$495(E) + 2 \times 320E(A_1) = 1135(E)$$

$$517(A_1) + 2 \times 320A_1(A_1) = 1157(A_1)$$

$$517(A_1) + 2 \times 320E(A_1) = 1157(A_1)$$

The $(\nu_1 + \nu_2)$ combinations were outside the region of experimental observation. None of the absorptions indicated in the $(\nu_1 + 2\nu_2)$ group were definitely observed.

$(v_1 + 3v_2)$

$495(F_{1u}) + 3 \times 320F_{1u} = 1455$ (not allowed)

$495(E) + 3 \times 320A_1(A_1) = 1455(E)$

$495(E) + 3 \times 320E(E) = 1455(A_1)$

$517(A_1) + 3 \times 320E(E) = 1477(E)$

$517(A_1) + 3 \times 320A_1(A_1) = 1477(A_1)$

The 1455 cm^{-1} absorption of the $(v_1 + 3v_2)$ group is not allowed in the cubic phase. This agrees with the experimental evidence. The two E symmetry combinations of the tetragonal phase are evidently weak.

$(v_1 + 3v_3)$

$495(F_{1u}) + 3 \times 265F_{1u} = 1290$ (not allowed)

$495(E) + 3 \times 265A_1(A_1) = 1290(E)$

$495(E) + 3 \times 265E(E) = 1290(A_1)$

$517(A_1) + 3 \times 265E(E) = 1312(E)$

$517(A_1) + 3 \times 265A_1(A_1) = 1312(A_1)$

From the $(v_1 + 3v_3)$ group, the 1290 cm^{-1} absorption is not allowed in the cubic phase, but this absorption exists in the tetragonal phase with A_1 symmetry. The E symmetry absorption is not observed. The 1312 cm^{-1} absorptions may account for the broader left edge of the observed absorption.

$(v_1 + 4v_3)$

$495(F_{1u}) + 4 \times 265F_{1u} = 1555(F_{1u})$

$495(E) + 4 \times 265E(A_1) = 1555(E)$

$495(E) + 4 \times 265A_1(A_1) = 1555(E)$

$517(A_1) + 4 \times 265E(A_1) = 1577(A_1)$

$517(A_1) + 4 \times 265A_1(A_1) = 1577(A_1)$

The $(v_1 + 4v_3)$ group is probably not useful since it involves the fourth harmonic of v_3 and should be very weak.

$(2v_1 + v_2)$

$2 \times 495F_{1u} + 320(F_{1u}) = 1310(F_{1u})$

$2 \times 495E(A_1) + 320(E) = 1310(E)$

$2 \times 495E(A_1) + 320(A_1) = 1310(A_1)$

$2 \times 517A_1(A_1) + 320(E) = 1354(E)$

$2 \times 517A_1(A_1) + 320(A_1) = 1354(A_1)$

The $(2v_1 + v_2)$ combinations may help to account for the broader left edge of the observed 1250 cm^{-1} absorption.

$(2v_1 + 2v_2)$

$2 \times 495F_{1u} + 2 \times 320F_{1u} = 1630$ (not allowed)

$2 \times 495E(A_1) + 2 \times 320E(A_1) = 1630(A_1)$

$2 \times 495E(A_1) + 2 \times 320A_1(A_1) = 1630(A_1)$

$2 \times 517A_1(A_1) + 2 \times 320E(A_1) = 1674(A_1)$

$2 \times 517A_1(A_1) + 2 \times 320A_1(A_1) = 1674(A_1)$

Nothing is observed to account for combinations of the $(2v_1 + 2v_2)$ group.

$(2v_1 + v_3)$

$2 \times 495F_{1u} + 265(F_{1u})\ = 1255(F_{1u})$

$2 \times 495E(A_1) + 265(E)\ = 1255(E)$

$2 \times 495E(A_1) + 265(A_1)\ = 1255(A_1)$

$2 \times 517A_1(A_1) + 265(E)\ = 1299(E)$

$2 \times 517A_1(A_1) + 265(A_1)\ = 1299(A_1)$

$(2v_1 + 2v_3)$

$2 \times 495F_{1u} + 2 \times 265F_{1u}\qquad = 1520\ (\text{not allowed})$

$2 \times 495E(A_1) + 2 \times 265E(A_1)\ = 1520(A_1)$

$2 \times 495E(A_1) + 2 \times 265A_1(A_1)\ = 1520(A_1)$

$2 \times 517A_1(A_1) + 2 \times 265E(A_1)\ = 1564(A_1)$

$2 \times 517A_1(A_1) + 2 \times 265A_1(A_1) = 1564(A_1)$

The $(2v_1 + v_3)$ combinations check against experimental evidence except for $1255(A_1)$ and $1299(E)$, which must be too weak. The $(2v_1 + 2v_3)$ combinations, although presumably weak, agree completely with the experimental results, which indicate a broad, shallow band centered at 1492 cm^{-1} having A_1 symmetry.

$(v_2 + v_2)$

$2 \times 320F_{1u}\qquad\quad = 640\ (\text{not allowed})$

$320(E) + 320(E)\quad = 640(A_1)$

$320(A_1) + 320(A_1) = 640(A_1)$

$320(A_1) + 320(E)\quad = 640(E)$

$(v_2 + 2v_2)$

$3 \times 320F_{1u}$ $= 960(F_{1u})$

$320(A_1) + 2 \times 320E(A_1) = 960(A_1)$

$320(A_1) + 2 \times 320A_1(A_1) = 960(A_1)$

$320(E) + 2 \times 320E(A_1)$ $= 960(E)$

$320(E) + 2 \times 320A_1(A_1) = 960(E)$

The $(v_2 + v_2)$ group was not within the region of observation. The $(v_2 + 2v_2)$ group could account for the flat spot in the transmission curves at 960 cm^{-1}.

$(v_2 + 3v_2)$

$4 \times 320F_{1u}$ $= 1280$ (not allowed)

$320(E) + 3 \times 320E(E)$ $= 1280(A_1)$

$320(A_1) + 3 \times 320A_1(A_1) = 1280(A_1)$

$320(E) + 3 \times 320A_1(A_1)$ $= 1280(E)$

$320(A_1) + 3 \times 320E(E)$ $= 1280(E)$

$(2v_2 + 2v_2)$

$4 \times 320F_{1u}$ $= 1280$ (not allowed)

$2 \times 320E(A_1) + 2 \times 320E(A_1)$ $= 1280(A_1)$

$2 \times 320E(A_1) + 2 \times 320A_1(A_1) = 1280(A_1)$

$2 \times 320A_1(A_1) + 2 \times 320A_1(A_1) = 1280(A_1)$

The 1280(E) combinations of the $(v_2 + 3v_2)$ group are not observed. The $(2v_2 + 2v_2)$ group agrees completely with the experimental evidence. This combination of second harmonics seems more reasonable than the $(v_2 + 3v_2)$ group.

$$(3v_2 + 2v_3)$$

$$3 \times 320F_{1u} + 2 \times 265F_{1u} = 1490(F_{1u})$$

$$3 \times 320A_1(A_1) + 2 \times 265A_1(A_1) = 1490(A_1)$$

$$3 \times 320A_1(A_1) + 2 \times 265E(A_1) = 1490(A_1)$$

$$3 \times 320E(E) + 2 \times 265A_1(A_1) = 1490(E)$$

$$3 \times 320E(E) + 2 \times 265E(A_1) = 1490(E)$$

The $(3v_2 + 2v_3)$ group indicates an absorption in the cubic phase at 1490 cm^{-1} which must be weak. The E symmetry combinations in the tetragonal phase must also be weak. This is not surprising considering the high harmonics used.

Discussion of Combinations

From the results obtained by the use of the selection rules, it appears that the 1250 cm^{-1} absorption obtained in the cubic phase arises from the $(2v_1 + v_3)$ combination. The $(2v_1 + v_2)$ group may account for the broader left side of this absorption. In the tetragonal phase, under polarized light with the electric vector perpendicular to the optical axis, this absorption remains at 1250 cm^{-1}. Thus in the $(2v_1 + v_3)$ group the E character must be stronger than the indicated A_1 character. The shift to 1287 cm^{-1} of this absorption when the electric vector is parallel to the axis is best accounted for by the 1299(A_1) absorption in the $(2v_1 + v_3)$ group. The $(v_1 + 3v_3)$ group also contributes to this, as well as the entire $(2v_2 + 2v_2)$ group.

The 1492 cm^{-1}(A_1) absorption observed with the electric vector parallel to the optical axis is best accounted for by the $(2v_1 + 2v_3)$ and $(v_1 + 3v_2)$ groups.

48

General Discussion

The only absorption dip noted in the room-temperature transmission curves for unpoled crystals occurred very nearly at 1250 cm^{-1}. The small variation in the position of this absorption with temperature is no doubt due to changes in domain configuration. As stated previously, from the results of the polarization study it can be seen that this 1250 cm^{-1} absorption is of E symmetry. It is surprising that all the transmission curves of crystals with domains randomly oriented displayed such a predominance of the E character. It is true however, that some of the samples displayed an extremely shallow dip in the region of 1475 cm^{-1}. A partial explanation for the predominance of the E character in the tetragonal phase is that with some crystals a portion of the sample area was made up of c-domains, that is, domains with the optical axis perpendicular to the crystal face. In these domains only the E symmetry vibrations could be excited. This explanation is not entirely satis-factory however, since many of the crystals were randomly oriented, displaying few observable c-domains.

The slight flattening observed in the 1475 cm^{-1} area as the tempera-ture is lowered from above the Curie point and on down through the tetragonal phase may be caused by the domain configuration losing more and more of the E symmetry as the temperature is lowered. This is supported by the small shift of the 1250 cm^{-1} absorption toward shorter wavelengths observed simultaneously.

From the use of the selection rules it appears that the 1250 cm^{-1} absorption is partly derived from v_1, a vibration of the oxygen octa-hedron. The observed shift in the tetragonal phase under polarized light is in the same direction as the shift of v_1 observed by Last.

Also supporting the relation to v_1 is the fact that the shifts of the 1250 cm^{-1} absorption at the crystal transition points agreed in direction with the shifts of v_1 obtained by Last. No experimental data is presently available concerning the shifts of v_2 or v_3 with either polarized light or crystal transitions. The E vibration of the tetragonal phase and the absorption of the cubic phase were both essentially 1250 cm^{-1}. Assuming this absorption is mainly due to vibrations of the oxygen octahedron, this may be explained by the fact that the T_i - O_{II} distance at right angles to the polar axis differs only slightly from the T_i - O distance in the cubic phase.

A broad, weak absorption appeared in the 1475 cm^{-1} area upon transition to the orthorhombic structure and was strengthened further in the rhombohedral phase. This is thought to be caused by an increase of A_1 character of the randomly oriented domain structure, rather than being the appearance of a new band due to lessened degeneracy associated with the orthorhombic structure.

In conclusion it appears that the values of the fundamental frequencies v_2 and v_3 may require some revision. The value obtained by Last for v_2 was extrapolated from the results of powdered sample data and an accuracy of 25 cm^{-1} was attached. The Ba - (T_iO_3) vibration, v_3, was calculated from specific heat data. No degree of accuracy was given. It is felt that the value for v_2 should be decreased and that for v_3 increased. Magnitudes for these frequencies cannot be definitely assigned from the results of this investigation alone, but considering only the infrared-active vibrational modes, the experimental results reported here can best be fitted by assigning values of approximately 320 cm^{-1} to v_2 and 265 cm^{-1} to v_3.

Suggestions for Further Study

Low temperature work using etched samples would be desirable.
However, a smaller low temperature cell which could be used in conjunc-
tion with the microbeam condenser should be constructed. Information
on the type of cell employed by Last in his investigation should be
obtained.

The most desirable area for further work would be a polarized
light investigation of samples etched down to various thicknesses in
order to study in more detail the region of the present long wavelength
cutoff. For example, a flat area in the transmission curves was ob-
served at about 960 cm^{-1} using thin randomly oriented crystals. It
would be suspected that a strong absorption would appear at 990 cm^{-1}
using a poled crystal. This absorption could be the second harmonic
of v_1 and should occur when the electric vector is parallel to the
optical axis since this combination is of A_1 symmetry. However, if
this absorption were observed with E symmetry this would then probably
mean that it was due to the third harmonic of v_2. In this event a more
exact value of this frequency could be assigned.

An investigation of the Raman spectrum would give information con-
cerning the frequencies of the infrared-inactive modes of vibration of
the oxygen octahedron. Facilities for this type of measurement are not
presently available.

BIBLIOGRAPHY

1. Megaw, H. D. Ferroelectricity in Crystals. Methuen and Co., Ltd., 1957.

2. Mara, R. T., G. B. B. M. Sutherland, and H. V. Tyrell. "Infrared Spectrum of Barium Titanate," Phys. Rev. 96, 801-2 (1954).

3. Hilsum, C. " Infrared Transmission of Barium Titanate" J. Opt. Soc. Am. 45, 771-2 (1955).

4. Yatsenko, A. F. "The Optical Transmission of $BaTiO_3$" Sov. Phys. Tech. Phys. 2, 2257-8 (1957).

5. Horie, T., K. Kawabe, and S. Sawada. "Optical Behaviours of Multi-domain Single Crystal of $BaTiO_3$ in Dependence on Temperature" Phys. Soc. Jap. J. 9, 823-5 (1954).

6. Horie, T., Kawabe, and T. Iwai. "Optical Studies of Single Crystals of Barium Titanate and Tungsten Trioxide" Ann. Rept. Sci. Works Fac. Sci. Osaka 4, 45-77 (1956).

7. Yatsenko, A. F. "Infrared Absorption Spectra of Perovskite-type Ferroelectric Crystals" Izvest. Akad. Nauk. S.S.S.R., Ser. Fiz. 22, 1456-8 (1958).

8. Last, J. T. "Infrared-Absorption Studies on Barium Titanate and Related Materials" Phys. Rev. 105, 1740-50 (1957).

9. Last, J. T. "Preparation of Thin Single Crystals of $BaTiO_3$" Rev. Sci. Inst. 28, 720-1 (1957).

10. Northrip, J. W. II. Master's Thesis, Oklahoma State University, 1958 (Unpublished).

11. Remeika, J. P. "A Method for Growing Barium Titanate Single Crystals" J. Am. Chem. Soc. 76, 940-1 (1954).

12. Belski, A. J. Master's Thesis, Oklahoma State University, 1960 (Unpublished).

13. Merz, W. J. "The Electric and Optical Behavior of $BaTiO_3$, Single-Domain Crystals" Phys. Rev. 76, 1221-5 (1949).

14. Herzberg, G. H. Infrared and Raman Spectra, New York: D. Van Nostrand Co., Inc., 1945, pp. 122 ff.

15. Wilson, E. B., J. C. Decius, P. C. Cross. <u>Molecular</u> <u>Vibrations</u>
    New York: McGraw-Hill Book Co., 1955.

VITA

Kenneth M. Proctor

Candidate for the Degree of

Master of Science

Thesis: INFRARED TRANSMISSION OF BARIUM TITANATE

Major Field: Physics

Biographical:

Personal Data: Born in Jones, Oklahoma, February 6, 1934, the
    son of Lionel and Ruth Proctor.

Education: Attended elementary school in Jones, Oklahoma;
    graduated from Jones High School in 1952; received the
    Bachelor of Science degree from Central State College,
    Edmond, Oklahoma, in May, 1956; completed requirements
    for Master of Science degree in May, 1962.

Experience: Employed for two years by Boeing Airplane Co.,
    Wichita, Kansas, in the acoustics staff.

Organizations: Member of Sigma Pi Sigma.